SEPTEMBER, 1968 REPORT R-392

CSL COORDINATED SCIENCE LABORATORY

SIMULATION OF A WET PROCESS CEMENT ROTARY KILN

JAI HARI DALMIA

UNIVERSITY OF ILLINOIS – URBANA, ILLINOIS

This work was supported in whole by the joint Services Electronics Program (U.S. Army, U.S. Navy, and U.S. Air Force) under contract DAAB-070670C-0199.

ACKNOWLEDGMENT

The author expresses his thanks to Professor W. R. Perkins for his very valuable guidance. The author is also grateful to Professor R. A. Schmitz of the Department of Chemistry and Chemical Engineering for his assistance and suggestions, and to Mrs. V. Metze for her indispensable help in programming and running the digital computer.

TABLE OF CONTENTS

LIST OF FIGURES

I. INTRODUCTION

I.1. Background and Objectives

The cement industry is now more than fifty years old and the manufacturing process perhaps older than a century. Steps in the manufacture of cement involve mixing of certain calcareous and siliceous materials and sintering them at a high temperature to produce a material having high cementing properties. The equipment employed in the process has remained much the same since the manufacture of cement began on a large scale, but with the demand of cement ever growing, larger and more sophisticated equipment is needed today. The older machines depended much on the skill of the operators to control them, utilizing very little instrumentation and automatic control. The most important equipment in the cement manufacture is the kiln, which is used to sinter the mixture of calcareous and siliceous materials, called slurry. Vertical shaft kilns and rotary kilns have been developed for the purpose. Rotary kilns are by far more in use today, primarily because they can be controlled better. With kilns getting larger, it has become necessary to reduce their downtime for economic reasons. Today this is being achieved by use of on-line digital computers. In this thesis the rotary kiln has been chosen for study.

A rotary kiln is a combination of a dryer, calciner and a reactor. The boundary of each region in the kiln is difficult to define because of overlapping of physical and chemical reactions taking place in the kiln. Slurry is fed at one end (called the feed end) of the kiln, which is also the exit for the flue. At the discharge end of the kiln

is a cooler, which cools the sintered material (called clinker), and preheats the secondary air required for combustion in the kiln. In this thesis, feed and discharge ends of the kiln are defined as the two boundaries of the system.

The objective of this study is to investigate the steady-state and transient behaviors of the kiln. This is accomplished by simulating the system on a digital computer, revealing the interaction of variables and facilitating the design of controllers for the process.

The following section describes the cement manufacturing process in general, with particular emphasis on the rotary kiln.

In Chapter II the plant is described by mathematical equations after identifying the various process variables. The mathematical model describes the material and energy balance at any given instant and at any point in the kiln. These equations for the rotary kiln are first-order non-linear partial differential equations with time and position along the kiln length as independent variables.

Chapter III describes the steady-state and transient simulations of the mathematical model on a digital computer. The study of steady-state behavior requires conversion of above equations into first-order ordinary differential equations with position along the kiln length as independent variable. To investigate the transient behavior, the kiln is divided into a convenient number of small sections of suitable but equal length. For each section and for each variable generalized differential-difference equations are written by method described by Filipovich.[1] These equations are then solved to obtain the transient

solution for deterministic inputs. In this thesis, kiln behavior is investigated for step variation in one of the independent controllable variables, kiln rotational speed (and hence the velocity of solids in the kiln).

I.2. The Cement Manufacturing Process

Basically there are two manufacturing processes for cement, dry process and wet process. The difference between the two is that while the former uses dry slurry to be converted to clinker and then to cement, the latter uses wet slurry. Even with this difference, all the manufacturing equipment employed in the two methods are the same. Figure 1 illustrates the wet process schematically.

The diagram illustrates the various stages of manufacture together with the strategic points of sampling the raw materials, intermediate products and the finished product for quality control. The heart of the process is the conversion of slurry to clinker, because the clinker, when powdered, itself has the cementing properties. Gypsum is added (about 4-5%) mainly to retard the setting rate of cement to a specific value as determined by various tests. Hence, the most important problem is to control the chemical composition of clinker within specified limits if cement is to be of standardized quality (by the term cement is meant "Portland Cement"). This further necessitates uniform quality of slurry and its proper burning in the rotary kilns.

Coming to the process itself, the basic raw materials for slurry are limestone, ferrite and clay. Limestone is usually obtained

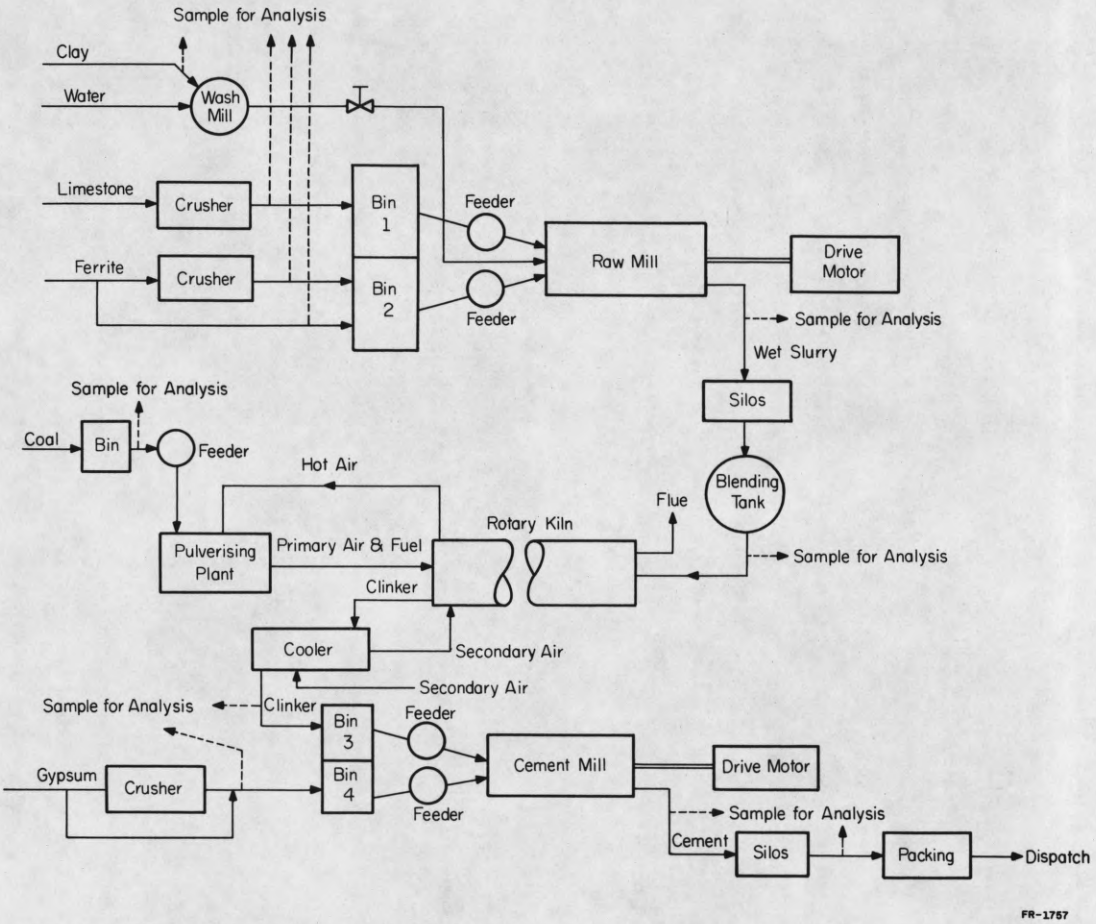

Figure 1. Flow diagram of cement manufacture by wet process.

in big lumps and is therefore crushed to required size and stored. Ferrite (used as a fluxing agent) is sometimes obtained in lumps and therefore needs crushing too, but this may be bypassed if received in small sizes. Clay, obtained from the fields, is passed through a washmill to remove undesired impurities. In dry process, clay is directly stored in bins for further processing and no water is added either before or later. The raw materials are fed into a raw mill (tubular mill driven by a motor) in controlled proportions by the feeders. The output of the mill is the slurry, which is first stored in silos and then blended in a blending tank. Blending is of utmost importance since the quality of clinker depends on its uniform quality. Furthermore, blending is necessary as the various raw materials, obtained from different sources, vary in their chemical compositions, e.g. limestone, obtained from two or three sources will never be identical in its chemical composition. Therefore uniform quality of slurry is obtained only if, in addition to chemical composition and adequate fineness of the raw mixture, the materials are carefully blended.

The slurry is then dried, calcined and sintered in a rotary kiln to clinker. This is now mixed with gypsum for the reason already mentioned. The mixture is then ground in a cement mill (similar to raw mill) to a fine powder and the final product so obtained is called cement.

The technology of the manufacturing process in the rotary kiln is based on the principle of heat exchange by counter-flow of material and heat. The mode of transmission of heat is the flue produced as a result of combustion.

Slurry is fed at one end of the kiln which is the exit end of the flue (see Fig. 2). Slurry feeder motor (not shown in the figure) gets electrical power from a generator coupled to the shaft of the kiln drive motor, and it therefore maintains the slurry feed per revolution of the kiln at a constant value.

As the kiln rotates at a very slow rate (about 1 to 2 mins/rev.), the material advances, and as it moves in the drying zone (which contains special heat economizing elements like chains and crosses) it is dried and converted to granules. The size of granules is important in the ultimate fusion of the material and hence of clinker. For this reason it is important to record the temperature (t_1) in this zone continuously. This temperature is about 700-800^{o}C. The granules are calcined as they move through the calcining zone and start fusing as they enter the sintering (or burning) zone. This is another important zone of the kiln for it is here that the material is completely burnt and converted to clinker. Any variation in temperature of this zone seriously affects the clinker quality, which as a result of poor temperature control may be overburnt or underburnt. For optimum burning it is therefore very important that the temperature be maintained constant and that the material may remain in this zone for a specified period. In this regard proper air-fuel ratio and flame length are also of importance. The former determines the optimum combustion of fuel and sintering of the material, and the latter determines the position and length of the sintering zone. To control the flame length and hence the flame height it is necessary to measure the hood pressure (P_h). Hood temperature (t_h) is

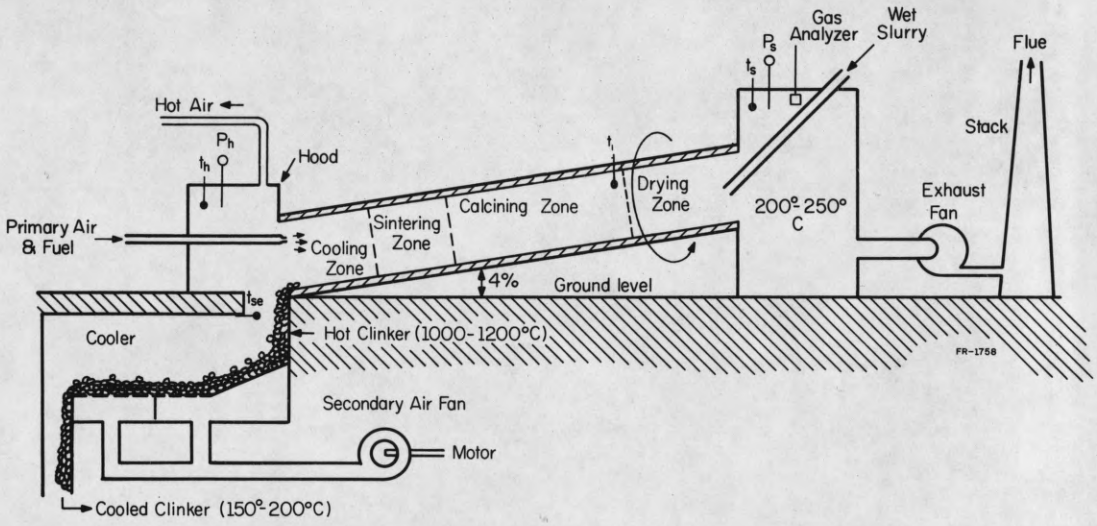

Figure 2. Rotary kiln with Folax Cooler.

maintained at a value to prevent the coal in the stream of air from igniting at the mouth of the nozzle itself.

The measure of draught pressure (P_s) in the smoke chamber enables to control the suction through the kiln and hence the temperature gradient along the kiln length. The temperature (t_s) in the smoke chamber is measured to assure that it is well above the dew point of the flue. Suction through the kiln is maintained by an induced draught fan (also called exhaust fan), which then lets the flue out through the stack. The draught near the exit is usually controlled by dampers (not shown).

The sintered material falls on a reciprocating (or travelling) grate of clinker cooler. Secondary air for combustion is forced through the grate and clinker bed. In the process the air itself gets preheated while cooling the clinker. This economizes heat requirement for clinker production.

While it is important to maintain the clinker quality, also of importance are to keep fuel consumption per unit weight of clinker produced at a minimum, and minimize the disturbance in the kiln. The most serious disturbance is temperature, which reduces the working life of fireproof refractories and hence may increase the downtime, thus affecting production. Another important effect of temperature variation is the ring formation in between calcining and sintering zones, which retards the material's advance and seriously disturbs its heat treatment. This may also lead to shutting down of the kiln.

A measure of optimum combustion is the air-fuel ratio, which depends on the calorific value of the fuel used (in this case coal). As in all combustion processes a slight excess air is always supplied to ensure complete combustion. An indication of this is the oxygen percentage by volume in the exhaust flue. This value seldom increases 4% but anywhere between 1-2% is a good indication of complete combustion. It is continuously measured by an automatic gas analyzer in the smoke chamber (Fig. 2). A frequent measurement of $\%CO_2$ by volume is also helpful. This is between 30-32%. Besides the air-fuel ratio, a certain amount of heat is to be supplied to the material for conversion to clinker and this comes mainly from fuel, however, this can be kept to a minimum by preheating the air (Fig. 2). The temperature of the primary air is limited to prevent ignition of fuel in the firing pipe itself, however, since the secondary air, preheated in the cooler, is supplied quite separately from the primary air, its temperature can be varied by altering grate speed. The amount or volume of secondary and primary air can be altered by means of dampers (not shown in Fig. 2) in their respective pipe lines. The link between fuel amount and combustion air can be altered via exhaust gas analysis.

Another chief quality index for clinker is the weight per unit volume, which is about 1450 (kg/m^3) for rotary kilns working on wet process. This index can be used to correct the temperature of the sintering zone in the kiln.

II. MATHEMATICAL MODEL OF THE KILN

The nature of a mathematical model for a system depends on how the system variables are defined, the boundary of the system is chosen for study, and the objectives the model is required to fulfill. Various kinds of process models are[2]:

a. Procedural model

b. Computational model

   (i) Inferential model

   (ii) Predictive model

      (1) Steady-state model

      (2) Dynamic model.

Each of the above models is briefly discussed below:

A procedural model consists of a set of instructions to be executed under predetermined situations. It is not a mathematical model and is formed on the basis of previous experiences of plant operators.

The inferential model infers the value of an unmeasured variable knowing the current values of the measured ones, with the help of certain mathematical relations either derived empirically or from natural laws. It is used where the unmeasured variable is important in the overall control of the system.

A predictive model has the capability of foreseeing the result of a control action. This type of model relates the input and output variables by mathematical equations and therefore has the ability to predict the outcome with perturbation in input variable(s). This model is widely used because of its effective control strategy. The predictive

model is subdivided into steady-state and dynamic models. The former describes the system behavior as time approaches infinity, while the latter is used to analyze the transient behavior of the system. Both steady-state and dynamic models can be used in the control of industrial processes. The former is used where perturbations are few and low in frequency, the system response to disturbances is fast, and for most of the time the system variables remain at steady-state. The dynamic control, on the other hand, becomes a necessity for a process (or system) which exhibits large time lags to disturbances, perturbation frequency is high, and the system variables remain more in the transient conditions. As it will be seen later, the rotary kiln requires a dynamic control.

In this thesis a predictive model is used to study the kiln behavior under both steady-state and transient conditions. But before such a model can be developed, it is essential to identify the process or system variables for their proper relationship. This is described in the following section.

II.1. The Process Variables

In any process, the variables can be distinguished as follows:[3]

(1)	Independent	a. Directly controllable	Temperatures, pressures, air and Liquid flow rates, etc., applied to the process.
		b. Uncontrollable	Composition of raw material, power generation loads, ambient temperature, catalyst deterioration, etc.

(2)	Dependent	Controllable only by manipulating independent variables	Temperatures, pressures, concentrations, etc., <u>that result within the process</u>.

<u>Independent variables</u> can be described as variables <u>that cause process behavior</u>; <u>dependent variables</u> as the <u>effects</u>. Independent variables are inputs to the process; dependent variables are in part the results of those inputs.

In the manual control of sintering in the kiln, the operator controls many variables: temperature, pressure, flow, etc. The interaction of certain variables together with their effect on other variables in the process is briefly discussed below. The dependent variable kiln temperature is examined:

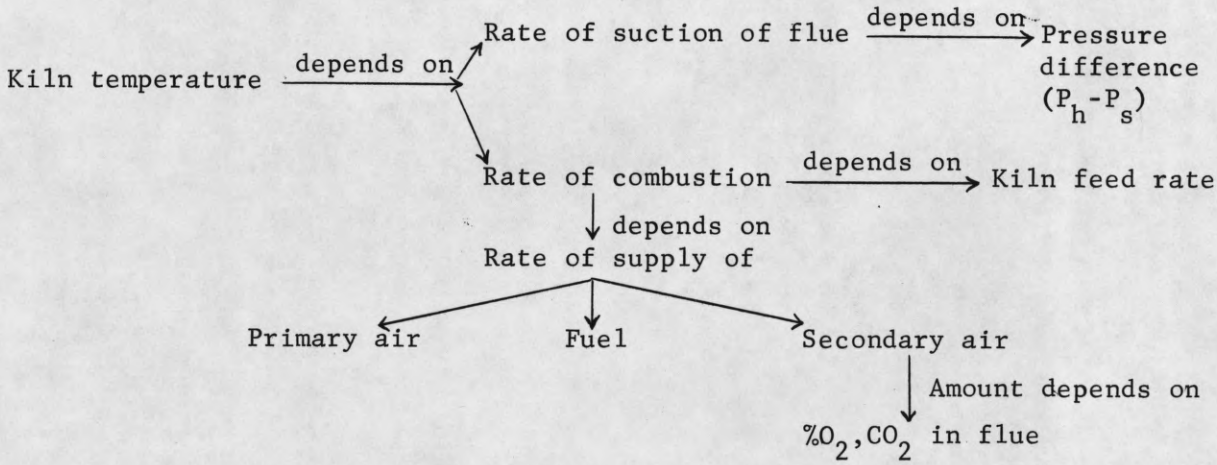

All these factors have been discussed in the previous chapter.

The control function, either manual or automatic, consists in regulating the controllable independent variables in a process to compensate for disturbances caused by uncontrollable variables such as, composition of kiln feed, fuel, etc., so that process objectives are continuously achieved.

The various process variables in the kiln and their nature are described below:

(1) Independent	a.	Directly controllable	Rate of flow of secondary air, fuel, and primary air; kiln speed (and hence flow of material in the kiln), rate of suction of flue.
	b.	Uncontrollable	Composition of fuel and kiln feed (slurry), ambient temperature.
(2) Dependent		Controllable only by manipulating independent variables.	Composition of clinker, temperatures of solids and gas.

Besides compensating for the disturbances, the control should be such that the dependent variables are within the constraints applied. For example, constraints on certain constituents of clinker to ensure its uniform quality, and constraints on temperatures of solids and gas to limit the heat losses may be imposed.

Figure 3 shows the kiln as a system with multiple inputs and outputs. In the figure the following notation is used:

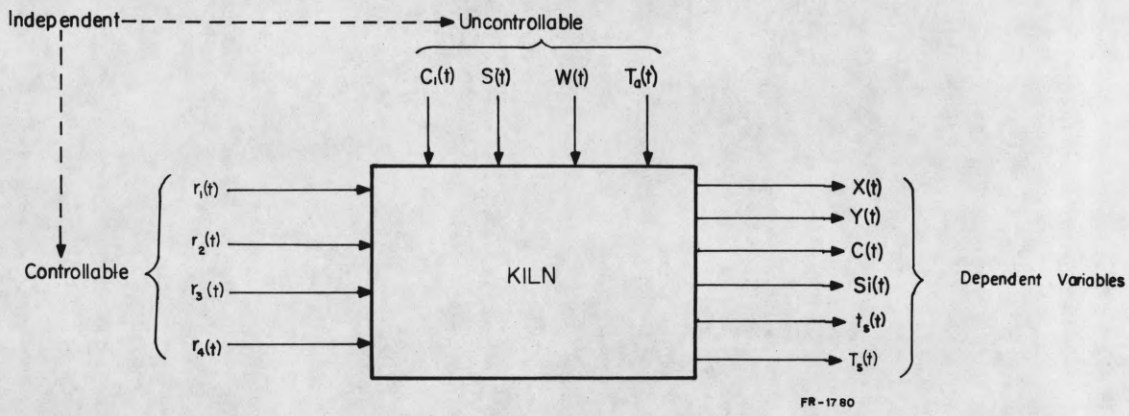

Figure 3. Block diagram of kiln with multiple inputs and outputs.

$r_1(t)$-------- Flow rate of primary air

$r_2(t)$-------- Flow rate of fuel

$r_3(t)$-------- Kiln rotational speed

$r_4(t)$-------- Flow rate of secondary air

$C_1(t), S(t), W(t)$-------- Concentrations of slurry

$X(t), Y(t)$-------- Concentrations of clinker

$C(t), Si(t)$-------- Concentrations of clinker

T_s-------- Solids temperature at discharge end of the kiln

T_a-------- Ambient temperature

t_s-------- Gas temperature at the feed end of the kiln.

II.2. Development of Dynamic Equations

The dynamic behavior of a system can be described basically in two ways: by input-output relationships, and by using the state-variable representation. The latter is more in use today because of its easy computer adaptibility, but it must be mentioned that this formulation is not unique as it depends on the way the system state-variables are selected.

In this study, the state-variable approach is used to formulate the mathematical model of the rotary kiln. One way of doing so for a chemical process such as this is to relate the various variables by means of material and energy (or heat) balance equations. The former are writtern from the stoichiometry of chemical reactions and the latter are developed from the first law of thermodynamics.

Such equations for the rotary kiln, without the constraints, are developed below. We introduce the following nomenclature:

A = Heat transfer area, (ft^2/ft)

A_i' = Rate constant, (1/hr)

B = Clinkerable mass/unit length, (lb/ft)

C = CaO/unit clinkerable mass, (lb/lb)

C_1 = CaO as $CaCO_3$/unit clinkerable mass, (lb/lb)

C' = CO_2/unit nitrogen mass, (lb/lb)

C_{p_g} = Specific heat of gas, (BTU/lb ^oF)

C_{p_s} = Specific heat of burden, (BTU/lb ^oF)

D = Kiln diameter, (m)

ΔE = Activation energy, (BTU/lb mole)

F = Fuel/unit nitrogen mass, (lb/lb)

f = Convective term, (BTU/hr ft^2 ^oF)

G_b = Clinkerable mass flow rate (solids only), (lb/hr)

G_g = Gass mass flow rate, (lb/hr)

G_n = Nitrogen mass flow rate, (lb/hr)

G_s = Burden mass flow rate (solids+water+CO_2), (lb/hr)

h = Heat transfer coefficient, (BTU/hr ft^2 ^oF)

H_i = Heat of reaction, (BTU/lb)

H_F = Calorific value of fuel, (BTU/lb)

k_i = Reaction rate coefficient, (1/hr)

ℓ = Kiln length, (m)

L = Distance from feed end, (ft)

M = Molecular weight

M_g = Gas mass/unit length, (lb/ft)

M_s = Burden mass/unit length, (lb/ft)

N = Nitrogen mass/unit length, (lb/ft)

ϕ = Oxygen/unit nitrogen mass, (lb/lb)

R = Gas constant, (BTU/^{o}R lb mole)

RF = Rate of combustion/unit nitrogen mass, (lb fuel/lb N_2 hr)

RW = Rate of evaporation/unit clinkerable mass, (lb H_2O/lb hr)

S = SiO_2/unit clinkerable mass, (lb/lb)

τ = Residence time of slurry in the kiln, (hr)

τ_o = Time for one rotation of kiln, (hr)

t = Real time, (hr)

T_a = Ambient temperature, (^{o}R)

T_g = Gas temperature, (^{o}R)

T_s = Burden temperature, (^{o}R)

T_w = Inside wall temperature, (^{o}R)

$T_{w'}$ = Outside wall (kiln shell) temperature, (^{o}R)

W = Water/unit clinkerable mass, (lb/lb)

W' = Water/unit nitrogen mass, (lb/lb)

X = $(CaO)_2SiO_2$/unit clinkerable mass, (lb/lb) (Symbolized as C_2S)

Y = $(CaO)_3SiO_2$/unit clinkerable mass, (lb/lb) (Symbolized as C_3S)

ϵ = Emissivity

α = Angle of inclination of kiln

Various chemical and physical reactions[4] taking place in the kiln are:

$$\text{Slurry } (50^{\circ}F) \xrightarrow{k_w} \text{Dry solids } (212^{\circ}F) - H_w \quad \text{(Drying)}$$

$$\text{Solids } (212^{\circ}F) \longrightarrow \text{Solids } (1650^{\circ}F) \quad \text{(Heating)}$$

$$CaCO_3 \xrightarrow{k_c} CaO + CO_2 - H_c \quad \text{(Calcining)}$$

$$\left.\begin{aligned} 2CaO+SiO_2 &\xrightarrow{k_x} (CaO)_2SiO_2 + H_x \\ (CaO)_2SiO_2+CaO &\xrightarrow{k_y} (CaO)_3SiO_2 - H_y \end{aligned}\right\} \quad \text{(Clinkering)}$$

Basically the dynamic equations we seek represent material and energy balance for solids and gas at any point in the kiln. The following assumptions are made to simplify the equations:

(i) No solids transported with the gas.

(ii) Minor compounds, such as iron and aluminium are neglected.

(iii) Specific heats, latent heats and heats of reactions are treated as constants.

(iv) Residence time is considered inversely proportional to the kiln speed.

(v) Velocity of a given particle of solids is constant throughout the kiln length.

(vi) All the fuel is burnt to CO_2.

We may then formulate the following equations:[5]

Material Balance

Solids

$$\frac{\partial C_1}{\partial t} = -k_c C_1 - \frac{G_b}{B} \frac{\partial C_1}{\partial L} \tag{II-1}$$

$$\frac{\partial C}{\partial t} = k_c C_1 - k_x C^2 S - k_y C X - \frac{G_b}{B} \frac{\partial C}{\partial L} \tag{II-2}$$

$$\frac{\partial S}{\partial t} = - \frac{M_S}{2M_C} k_x C^2 S - \frac{G_b}{B} \frac{\partial S}{\partial L} \tag{II-3}$$

$$\frac{\partial X}{\partial t} = \frac{M_X}{2M_C} k_x C^2 S - \frac{M_X}{M_C} k_y C X - \frac{G_b}{B} \frac{\partial X}{\partial L} \tag{II-4}$$

$$\frac{\partial Y}{\partial t} = \frac{M_Y}{M_C} k_y C X - \frac{G_b}{B} \frac{\partial Y}{\partial L} \tag{II-5}$$

$$G_s = G_b \left(1 + \frac{M_{C'}}{M_C} C_1 + W \right) \tag{II-6}$$

$$M_s = B \left(1 + \frac{M_{C'}}{M_C} C_1 + W \right) \tag{II-7}$$

Gas

$$\frac{\partial C'}{\partial t} = - \frac{M_{C'}}{M_F} RF - \frac{B}{N} \frac{M_{C'}}{M_C} k_c C_1 - \frac{G_n}{N} \frac{\partial C'}{\partial L} \tag{II-8}$$

$$\frac{\partial W'}{\partial t} = - \frac{2M_W}{M_F} RF - \frac{B}{N} RW - \frac{G_n}{N} \frac{\partial W'}{\partial L} \tag{II-9}$$

$$\frac{\partial \phi}{\partial t} = \frac{2M_\phi}{M_F} RF - \frac{G_n}{N} \frac{\partial \phi}{\partial L} \tag{II-10}$$

$$G_g = G_n (1 + \phi + W' + C' + F) \tag{II-11}$$

$$M_g = N(1 + \phi + W' + C' + F) \tag{II-12}$$

Energy balance

$$C_{p_s} M_s \frac{\partial T_s}{\partial t} = \left[h_2 A_2 (T_g - T_s) + h_3 A_3 (T_w - T_s) - BH_c k_c C_1 - BH_w RW + BH_x k_y C^2 S - BH_y k_y CX - C_{p_s} G_s \frac{\partial T_s}{\partial L} \right] \quad \text{(II-13)}$$

$$C_{p_g} M_g \frac{\partial T_g}{\partial t} = \left[h_1 A_1 (T_g - T_w) + h_2 A_2 (T_g - T_s) - C_{p_s} (T_s - T_g) \frac{\partial G_s}{\partial L} + NH_F R_F - C_{p_g} G_g \frac{\partial T_g}{\partial L} \right] \quad \text{(II-14)}$$

$$T_w^{(6)} = \frac{h_1 A_1 (h_4 A_4 + h_5 A_5) T_g + h_3 A_3 (h_4 A_4 + h_5 A_5) T_s + h_4 A_4 \cdot h_5 A_5 \cdot T_a}{h_1 A_1 (h_4 A_4 + h_5 A_5) + h_3 A_3 (h_4 A_4 + h_5 A_5) + h_4 A_4 \cdot h_5 A_5} \quad \text{(II-15)}$$

$$T_{w'} = \frac{h_5 A_5 T_a + h_4 A_4 T_w}{h_5 A_5 + h_4 A_4} \quad \text{(II-16)}$$

Heat transfer coefficients[5]

$h_1 = f_1 + 3.4203 \times 10^{-9} \epsilon_g \epsilon_w (T_g^3 + T_w^3)$ (gas to inner wall) (II-17)

$h_2 = f_2 + 3.4203 \times 10^{-9} \epsilon_g \epsilon_s (T_g^3 + T_s^3)$ (gas to solids) (II-18)

$h_3 = f_3 + 3.4203 \times 10^{-9} \frac{A_2}{A_3} \epsilon_w \epsilon_s (T_w^3 + T_s^3)$ (inner wall to solids) (II-19)

$h_4 =$ constant (inner wall to outer wall) (II-20)

$h_5 = f_5 + 3.4203 \times 10^{-7} \epsilon_{w'} (T_{w'}^3 + T_a^3)$ (outer wall to ambient) (II-21)

Rates and rate constants[5]

$$k_i = A_i' \exp(-\Delta E / RT_s) \quad \text{(II-22)}$$

$$RW = k_w (W \geq 0.1) \quad \text{(II-23)}$$

$$= k_w W (W < 0.1) \quad \text{(II-24)}$$

$$RF = \frac{2F}{365 - L} \quad \text{(II-25)}$$

Equation (II-25) is the modified form of the one in the above reference and indicates that maximum combustion takes place at about 365 feet from the feed end.

Residence time[7]

$$\tau = \frac{\ell \tau_o}{0.0963 D\alpha} \qquad \text{(II-26)}$$

Thermodynamic and Other Data

Heats of reaction [5]

Nearly all chemical and physical reactions are accompanied by absorption (endothermic) or liberation (exothermic) of heat. This is dependent on the nature of the reactants and the resultants, and must be accounted for in energy balance (or heat balance) equations. For the reactions taking place in the kiln, the values of the heats of reaction are:

H_w	970 (BTU/lb)	Endothermic
H_c	1275 (BTU/lb CaO)	Endothermic
H_y	11 (BTU/lb CaO)	Endothermic
H_x	381 (BTU/lb CaO)	Exothermic

Specific Heats[5]

The specific heats of solids and gas vary along the kiln length as their concentrations and temperature change. To simplify the calculations, these values are assumed to be constant throughout

the kiln length and are the average values of the specific heats of their constituents.

C_{P_g}	0.28 (BTU/lb ^{o}R)
C_{P_s}	0.26 (BTU/lb ^{o}R)

Activation energies[5]

The rate of a chemical reaction, especially at high temperatures, is largely controlled by the activation energy. For the kiln reactions, these values are:

ΔE_W	18000 (BTU/lb mole)
ΔE_C	261000 (BTU/lb mole)
ΔE_X	83000 (BTU/lb mole)
ΔE_Y	110000 (BTU/lb mole)

Reaction rate constants

During the initial simulation, the values used for reaction rate constants were those suggested by Lyons,[5] but were adjusted in later simulations so that with the initial values given in the next chapter, the steady-state profiles conform as nearly as possible to those given by him. The final adjusted values are:

A'_W	3.9×10^{7} (1/hr)
A'_C	1.4×10^{37} (1/hr)
A'_X	2.62×10^{12} (1/hr)
A'_Y	2.8×10^{13} (1/hr)

Heat transfer coefficients and heat transfer area

During the initial simulation, values given by Lyons[5] were used but were adjusted for the same reason as reaction rate constants. Different values in some cases are due to different values of convective term 'f', heat transfer area 'A', and emissivity 'ϵ'. Since the values of f, A, and ϵ are included in heat transfer coefficient (Equations II-17 to II-21), their values are not given separately. The final adjusted values are:

h_1A_1	236 (BTU/M ^{o}R)	(118 in the last 50 feet)
h_2A_2	615 (BTU/M ^{o}R)	(28 in the last 50 feet)
h_3A_3	70 (BTU/M ^{o}R)	(31 in the last 50 feet)
h_4A_4	10 (BTU/M ^{o}R)	
h_5A_5	32 (BTU/M ^{o}R)	

Molecular weights

M_X	172	
M_C	56	
M_Y	228	
M_S	60	
$M_{C'}$	44	
M_F	16	(Fuel is assumed to be made up of CH_4)
M_W	18	
M_Φ	16	

Other data (taken from personal practical experience)

$l^{(4)}$	450 (ft) (= 137 m)
D	3.65 (m)
α	2.3^{o} (= 4%)
τ_o	1/60-1/120 (hr)
H_F	10800 (BTU/lb)

III. DIGITAL SIMULATION OF KILN

The objectives of the simulation are:

a. To obtain the gas and solids temperature profiles along the kiln length.

b. To obtain concentration profiles of important products formed as a result of reactions taking place in the kiln.

In obtaining these profiles the slurry feed end (Fig. 2) is taken as origin or reference. The profiles are obtained first for a given rotational speed of the kiln (and hence for a given residence time of slurry in the kiln), and then for step inputs to the rotational speed. The magnitude of the steps are determined by the upper and lower constraints on the rotational speed, stated in Chapter I.

III.1. Steady-state Simulation

Steady-state equations

To achieve the stated objectives, it is helpful to convert the dynamic model to a steady-state model, i.e., to ordinary differential equations with position along the kiln length (L) as the independent variable. For this, we let $t \rightarrow \infty$ and note that $\frac{\partial}{\partial t} \rightarrow 0$, so that at steady-state the dynamic equations reduce to the following steady-state equations after substituting the values of molecular weights and $w_o = G_b/B$:

Material balance

Solids

$$\frac{dC_1}{dL} = -\frac{1}{w_o} k_c C_1 \qquad \text{(III-1)}$$

$$\frac{dS}{dL} = -\frac{0.535}{w_o} k_x C^2 S \qquad \text{(III-2)}$$

$$\frac{dC}{dL} = -\frac{1}{w_o} [k_c C_1 - k_x C^2 S - k_y C X] \qquad \text{(III-3)}$$

$$\frac{dW}{dL} = -\frac{1}{w_o} RW \qquad \text{(III-4)}$$

$$\frac{dX}{dL} = \frac{1.536}{w_o} [k_x C^2 S - 2.0 k_y C X] \qquad \text{(III-5)}$$

$$\frac{dY}{dL} = \frac{4.07}{w_o} k_y C X \qquad \text{(III-6)}$$

$$G_s = G_b(1+0.786C_1+W) \qquad \text{(III-7)}$$

Gas

Let $w_g = G_n/N$ = Gas velocity, then

$$\frac{dC'}{dL} = -\frac{1}{w_g} [2.75\ RF + 0.786\ \frac{B}{N}\ k_c C_1] \qquad \text{(III-8)}$$

$$\frac{dW'}{dL} = -\frac{1}{w_g} [2.25\ RF + \frac{B}{N}\ RW] \qquad \text{(III-9)}$$

$$\frac{d\phi}{dL} = \frac{2RF}{w_g} \qquad \text{(III-10)}$$

$$G_g = G_n(1+\phi+W' + C' + F). \qquad \text{(III-11)}$$

Energy balance

Let $\beta_j = h_j A_j (j = 1,\ldots,5)$. Then

$$\frac{dT_s}{dL} = \frac{1}{C_{p_s} G_s}\left[\beta_2(T_g - T_s) + \beta_3(T_w - T_s) - B(H_c k_c C_1 - H_x k_x C^2 S + H_y k_y CX + H_w RW)\right] \quad \text{(III-12)}$$

$$\frac{dT_g}{dL} = \frac{1}{C_{p_g} G_g}\left[\beta_1(T_g - T_w) + \beta_2(T_g - T_s) + C_{p_g}(T_g - T_s)\frac{dG_s}{dL} + NH_F RF\right] \quad \text{(III-13)}$$

Because the gas flows in opposite direction to solids, due regard to sign has been given in writing the material and energy balance equations for it. Furthermore, since in the last 50 feet heat is transmitted from solids and inner wall to the gas, Equations (III-12) and (III-13) become

$$\frac{dT_s}{dL} = \frac{1}{C_{p_s} G_s}\left[\beta_2(T_s - T_g) + \beta_3(T_w - T_s) - B(H_c k_c C_1 - H_x k_x C^2 S + H_y k_y CX + H_w RW)\right] \quad \text{(III-12a)}$$

$$\frac{dT_g}{dL} = \frac{1}{C_{p_g} G_g}\left[\beta_1(T_w - T_g) + \beta_2(T_s - T_g) + C_{p_g}(T_s - T_g)\frac{dG_s}{dL} + NH_F RF\right] \quad \text{(III-13a)}$$

$$T_w = \frac{\beta_1(\beta_4+\beta_5)T_g + \beta_3(\beta_4+\beta_5)T_s + \beta_4\beta_5 T_a}{\beta_1(\beta_4+\beta_5) + \beta_3(\beta_4+\beta_5) + \beta_4\beta_5} \quad \text{(III-14)}$$

$$T_{w'} = \frac{\beta_5 T_a + \beta_4 T_w}{\beta_5 + \beta_4} \quad \text{(III-15)}$$

Initial values and simulation results

In order that the simulation results be as practical as possible, common initial values of wet process rotary kilns, were used.

$C_1(t,0)$	0.67	(lb/lb)	(based on personal practical experience)
$S(t,0)$	0.33	(lb/lb)	(based on personal practical experience)
$C(t,0)$	0.0	(lb/lb)	(based on personal practical experience)
$W(t,0)$	0.837	(lb/lb)	(based on 32% moisture content in slurry)
$X(t,0)$	0.0	(lb/lb)	(based on personal practical experience)
$Y(t,0)$	0.0	(lb/lb)	(based on personal practical experience)
$C'(t,0)$ [4]	0.381	(lb/lb)	
$W'(t,0)$ [4]	0.451	(lb/lb)	
$\phi(t,0)$ [4]	0.072	(lb/lb)	
G_b	55000	(lb/hr)	(based on 600 tons/day production)
G_n [4]	167300	(lb/hr)	
F	13750	(lb/hr)	(based on 25% of clinker production)
$T_g(t,0)$	950	(^oR)	(upper limit of constraint)
$T_s(t,0)$	510	(^oR)	(assumed)
$T_a(t)$	550	(^oR)	(assumed)
τ	3.5	(hrs)	(based on about 75 secs/rev of kiln)
w_g	925	(ft/hr)	(assumed)

With the above initial values, the mathematical model was simulated on a Control Data 1604 digital computer using Runge-Kutta-Gill's numerical method of solution for first order ordinary differential equations. The concentration and temperature profiles obtained are shown in Fig. 4. The following end results were obtained:

Initial values and simulation results

In order that the simulation results be as practical as possible, common initial values of wet process rotary kilns, were used.

$C_1(t,0)$	0.67	(lb/lb)	(based on personal practical experience)
$S(t,0)$	0.33	(lb/lb)	(based on personal practical experience)
$C(t,0)$	0.0	(lb/lb)	(based on personal practical experience)
$W(t,0)$	0.837	(lb/lb)	(based on 32% moisture content in slurry)
$X(t,0)$	0.0	(lb/lb)	(based on personal practical experience)
$Y(t,0)$	0.0	(lb/lb)	(based on personal practical experience)
$C'(t,0)$ [4]	0.381	(lb/lb)	
$W'(t,0)$ [4]	0.451	(lb/lb)	
$\phi(t,0)$ [4]	0.072	(lb/lb)	
G_b	55000	(lb/hr)	(based on 600 tons/day production)
G_n [4]	167300	(lb/hr)	
F	13750	(lb/hr)	(based on 25% of clinker production)
$T_g(t,0)$	950	(^oR)	(upper limit of constraint)
$T_s(t,0)$	510	(^oR)	(assumed)
$T_a(t)$	550	(^oR)	(assumed)
τ	3.5	(hrs)	(based on about 75 secs/rev of kiln)
w_g	925	(ft/hr)	(assumed)

With the above initial values, the mathematical model was simulated on a Control Data 1604 digital computer using Runge-Kutta-Gill's numerical method of solution for first order ordinary differential equations. The concentration and temperature profiles obtained are shown in Fig. 4. The following end results were obtained:

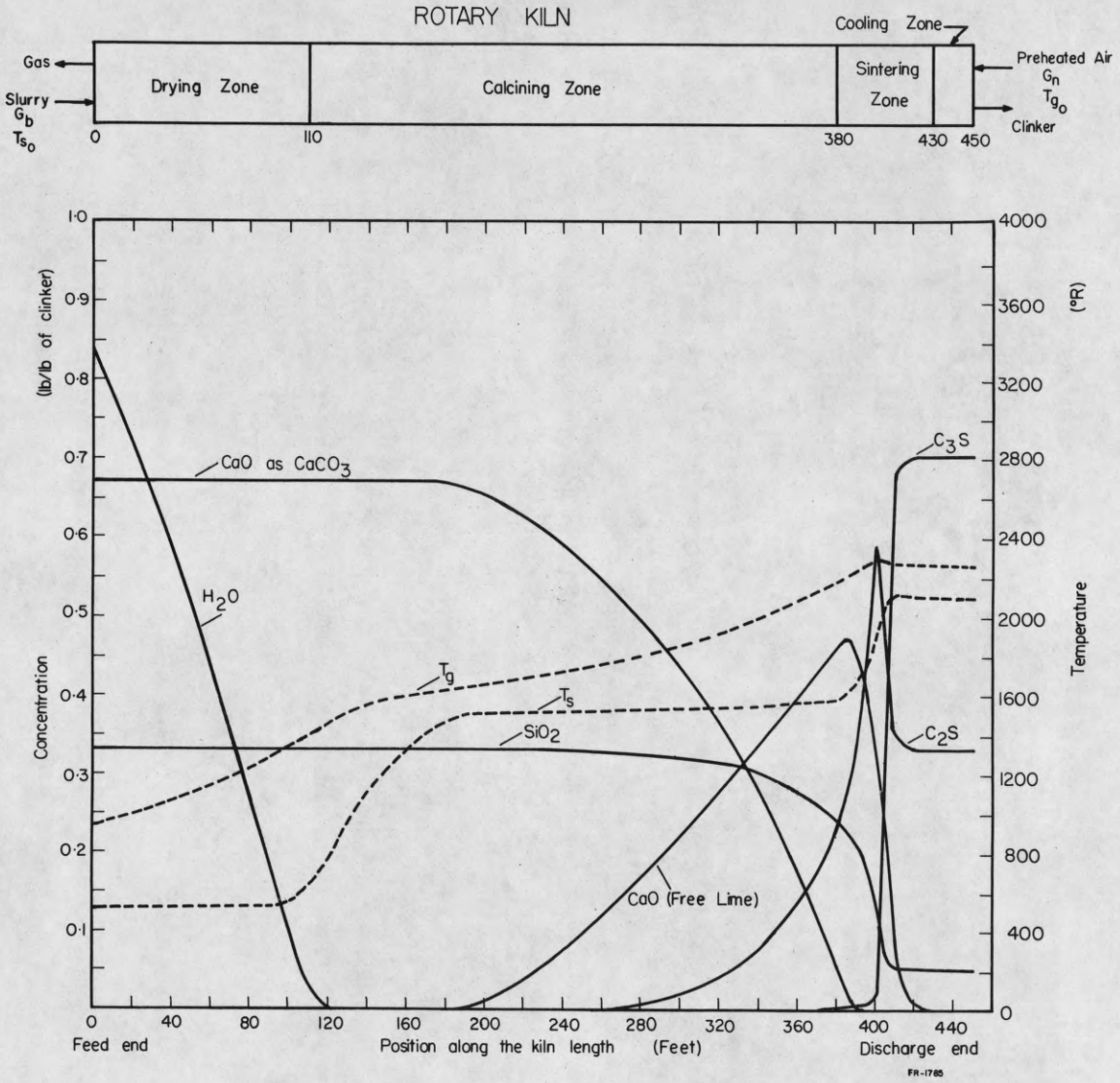

Figure 4. Steady-state temperature and concentration profiles along kiln length.

Clinker composition (lb/lb of clinker)

CaO (free lime)	SiO_2 (unreacted silica)	C_2S	C_3S
0.0	0.029	0.331	0.703

clinker temperature at discharge end

891.38 ^{o}C.

Discussion of simulation results

A theoretical mathematical model will not always give satisfactory practical results. Even in actual practice, before a model can be used for control of the process, adjustment in parameters is necessary until the deviation of simulation results from those observed in actual process is acceptable. In this simulation some parameters (already mentioned in the previous chapter) were adjusted until intermediate and end results conformed closely to those given by Lyons.[5]

The important intermediate and end results of simulation are given below against their practical values for comparison:

	Simulation value	Practical value
(1) C_3S	0.703	0.5-0.55[8]
(2) C_2S	0.331	0.2-0.25[8]
(3) C_3S/C_2S	2.12	2.20
(4) CaO (free lime)	0.0	0.0-0.001 (personal experience)

	Simulation value	Practical value	
(5) Approximate clinker temperature at discharge end	900 °C	1000-1200 °C	(personal experience)
(6) Approximate peak gas temperature	1000 °C	1200-1400 °C	(personal experience)
(7) Approximate peak kiln shell temperature	245 °C	220-250 °C	(personal experience)
(8) Approximate length of drying zone	110 ft	100 ft	(personal experience)
(9) Approximate length of calcining zone	270 ft	270 ft	(personal experience)
(10) Approximate length of sintering zone	50 ft	40 ft	(personal experience)

Deviation of the simulated results from practical values occurs because

(i) Assumptions listed previously are not rigorously true.

(ii) Values of heat transfer coefficients, gas velocity, air-fuel ratio are only assumed.

III.2. Transient Analysis

The objective of transient analysis is to obtain the shift of the boundaries of various zones as defined by the steady state profiles (Fig. 4), due to a step change in one of the controlled independent variables, kiln rotational speed (and hence the velocity of solids in the kiln).

The kiln is divided into forty five sections, each of 10 feet length (for more accurate results, more number of sections are used). For each section and for each variable of the solids' material balance equations, generalized differential-difference equations are written by the method described by Filipovich.[1] Variables, which have the same value, or change by a small amount in a particular section as compared to their value in the preceding one, do not have any equation for that section. Equation (II-1) would be used as an example to derive generalized differential-difference equations.

The dynamic equation is

$$\frac{\partial C_1}{\partial t} = -k_c C_1 - \frac{G_b}{B} \frac{\partial C_1}{\partial L}$$

let $G_b/B = w_o$, then

$$\frac{\partial C_1}{\partial t} + w_o \frac{\partial C_1}{\partial L} = -k_c C_1. \qquad \text{(III-16)}$$

We know

$$\frac{dC_1}{dt} = \frac{\partial C_1}{\partial t} + \frac{\partial C_1}{\partial L} \frac{dL}{dt}$$

or

$$\frac{\partial C_1}{\partial t} = \frac{dC_1}{dt} - \frac{\partial C_1}{\partial L} \frac{dL}{dt}.$$

Hence Equation (III-16) becomes

$$\frac{dC_1}{dt} + \frac{\partial C_1}{\partial L}\left(w_o - \frac{dL}{dt}\right) = -k_c C_1. \qquad \text{(III-17)}$$

Let the boundary of the region for C_1 be denoted by

$$C_1[t, L_{C_1}(t)] = 0$$

where $L = L_{C_1}(t)$ defines the boundary where calcination zone ends.

Boundary conditions are:

$$C_1[t,0] = C_1^{o}(t) = C_{1o} \text{ (constant)} \qquad (t \geq 0)$$

$$w[t,0] = w^{o}(t) = w_o + \Delta w^{o}(t) \qquad (t \geq 0)$$

$$C_1[0,L] = f_2(L) = {}^{o}C_{1j}$$

where

$$\Delta w^{o}(0) = 0$$

$$w^{o}(t) > 0,$$

and where $f_2(L)$ is the steady-state which would be obtained at the instant t=0, with the following conditions:

$$C_1[t,0] = C_{1o} = \text{constant} \qquad (t \leq 0)$$

$$w[t,0] = w_o = \text{constant} \qquad (t \leq 0).$$

Generalizing the Equation (III-17) for any boundary $L = L_j(t)$, we have

$$\frac{dC_{ij}}{dt} + \left(\frac{\partial C_1}{\partial L}\right)_{L=L_j(t)} \left(w_o - \frac{dL_j}{dt}\right) = -k_{cj} C_{ij} \qquad \text{(III-18)}$$

where

$$C_{1j} = C_1[t, L_j(t)]$$

$$\frac{dL_j}{dt} \neq \infty .$$

If for a family of curves $L = L_j(t)$ the error of approximation

$$\left(\frac{\partial C_1}{\partial L}\right)_{L=L_j(t)} \approx \frac{C_{ij} - C_{ij-1}}{L_j - L_{j-1}}$$

is sufficiently small, then (III-18) becomes

$$\frac{dC_{1j}}{dt} + \frac{C_{1j}-C_{1j-1}}{L_j-L_{j-1}}\left(w_o - \frac{dL_j}{dt}\right) = -k_{cj}C_{1j} \quad (j=17,\ldots,39). \qquad \text{(III-19)}$$

If the curves are defined as $\frac{dC_{1j}}{dt} = 0$, i.e. the value of the variable C_1 at the boundary of the region of definition remains constant, then curves $L = L_j(t)$ become level contours. Applying this condition and rearranging (III-19) we get

$$\frac{dL_j}{dt} = w_o + k_{cj}C_{1j}\frac{L_j-L_{j-1}}{C_{1j}-C_{1j-1}} . \qquad \text{(III-20)}$$

Similar equations can be derived for other variables of the solids material balance equations. They are listed below:

$$\frac{dL_j}{dt} = w_o + 0.535\, k_{xj}C_j^2 S_j \frac{L_j-L_{j-1}}{S_j-S_{j-1}} \qquad \text{(III-21)}$$

$$\frac{dL_j}{dt} = w_o + RW_j \frac{L_j-L_{j-1}}{W_j-W_{j-1}} \qquad \text{(III-22)}$$

$$\frac{dL_j}{dt} = w_o - 1.536\left[k_{xj}C_j^2 S_j - 2.0k_{yj}C_jX_j\right]\frac{L_j-L_{j-1}}{X_j-X_{j-1}} \qquad \text{(III-23)}$$

$$\frac{dL_j}{dt} = w_o - 4.0\, k_{yj}C_jX_j \frac{L_j-L_{j-1}}{Y_j-Y_{j-1}} . \qquad \text{(III-24)}$$

It will be observed that variable 'C' is left out because at the end of sintering zone its value is zero and is totally converted to X and Y in reacting with 'S'. Therefore, the end of sintering zone can be defined by concentrations of X, Y, and S only. However, such a

situation does not arise in defining the end of drying zone because no intermediate products are formed here and 'W' is the only variable. In calcining zone, together with calcination of $CaCO_3$ (denoted by C_1), intermediate products are also formed. However, since only one chemical reaction (calcination of $CaCO_3$) is completed it is convenient to define the end of this zone at the point where $CaCO_3$ (or variable C_1) reduces to zero.

Equations (III-20) to (III-24) can be written as a system of generalized differential-difference equations for variation of contour lines with respect to their steady-state position as

$$\frac{d\Delta L_j}{dt} - a_j \Delta L_j = \Delta w^o - a_j \Delta L_{j-1} \quad (j=1,\ldots,45) \qquad \text{(III-25)}$$

with the initial conditions

$$L_j(0) = 0$$

and

$$\Delta L_o = 0, \; \Delta L_j = L_j(t) - L_j(0) \qquad (j = 1,\ldots,45)$$

$$L_j(0) = f_1^{-1}({}^oW_j) \qquad (j = 1,\ldots,12)$$

$$L_j(0) = f_2^{-1}({}^oC_{1j}) \qquad (j = 17,\ldots,21)$$

$$L_j(0) = f_3^{-1}({}^oC_{1j}, {}^oS_j, {}^oX_j) \qquad (j = 22,\ldots,33)$$

$$L_j(0) = f_4^{-1}({}^oC_{1j}, {}^oS_j, {}^oX_j, {}^oY_j) \qquad (j = 34,\ldots,39)$$

$$L_j(0) = f_5^{-1}({}^oS_j, {}^oX_j, {}^oY_j) \qquad (j = 40, 41)$$

Let

$$\alpha_j = RW_j/(W_j - W_{j-1}) \qquad \text{(III-26)}$$

$$\delta_j = k_{cj}C_{1j}/(C_{1j} - C_{1j-1}) \qquad \text{(III-27)}$$

$$\nu_j = 0.535\, k_{xj}C_j^2 S_j/(S_j - S_{j-1}) \qquad \text{(III-28)}$$

$$\mu_j = -1.536\, [k_{xj}C_j^2 S_j - 2.0k_{yj}C_jX_j]/(X_j - X_{j-1}) \qquad \text{(III-29)}$$

$$\lambda_j = -4.0k_{yj}C_jX_j/(Y_j - Y_{j-1}) \qquad \text{(III-30)}$$

then

$$a_j = \begin{cases} \alpha_j & (j = 1,\ldots,12) \\ \delta_j & (j = 17,\ldots,21) \\ \delta_j, \nu_j, \mu_j & (j = 22,\ldots,33) \\ \delta_j, \nu_j, \mu_j, \lambda_j & (j = 34,\ldots,39) \\ \nu_j, \mu_j, \lambda_j & (j = 40, 41)\ . \end{cases}$$

The values of a_j's for each section are calculated by substituting the respective values of k's, concentrations and temperatures obtained in steady state analysis, in (III-26) to (III-31). The calculated values are tabulated below:

	a_j's				
j	α_j	δ_j	ν_j	μ_j	λ_j
1	-12.91				
2	-13.18				
3	-13.20				
4	-13.19				

	a_j's				
j	α_j	δ_j	ν_j	μ_j	λ_j
5	-13.19				
6	-13.17				
7	-13.21				
8	-13.20				
9	-13.19				
10	- 4.19				
11	- 1.35				
12	0				
17		-16.10			
18		-40.35			
19		-29.10			
20		-15.91			
21		-13.48			
22		-13.7	-10.89	-14.2	
23		-13.3	-21.6	-17.2	
24		-13.39	-18.8	-16.6	
25		-13.3	-15.13	-16.05	
26		-13.34	-15.33	-15.62	
27		-13.39	-14.97	-15.32	
28		-13.37	-15.99	-15.32	
29		-13.39	-14.64	-14.83	
30		-13.33	-15.29	-14.82	
31		-13.4	-14.8	-14.75	
32		-13.38	-13.91	-14.19	
33		-13.38	-14.5	-14.52	
34		-13.39	-14.42	-14.46	- 6.57
35		-13.31	-14.4	-14.4	-15.2
36		-13.36	-14.2	-14.32	-16.52
37		-13.8	-14.75	-14.72	-16.3
38		-13.2	-15.36	-15.23	-17.96

	a_j's				
j	α_j	δ_j	ν_j	μ_j	λ_j
39		-49.5	-17.65	-17.6	- 24.25
40		0	-42.8	-33.36	-136.4
41			- 0.03	- 2.19	- 1.23

The missing a_j's and j's correspond to sections where there is either a very small change or no change in the value of the variable as compared to its value in the preceding section.

Now, these values of a_j's are substituted in equation (III-25) and solved for L_j, with j = 11, 39, and 41, which respectively define the boundaries of drying, calcining and sintering zones, for a positive step, $\Delta w^o = w_o/4.3$ and for a negative step, $\Delta w^o = -w_o/2.6$.

Discussion of simulation results

The steady-state concentrations and temperatures profiles after the positive and negative steps are shown in Figures 5 and 6, respectively. Figure 5 shows that the shift in the boundary of the drying zone (where moisture content is about 0.03 (lb/lb of clinker) is independent of the interaction of any other process variable. It should be mentioned here that in the transient analysis no variation in the values of gas and solids' temperatures is assumed. But Fig. 6 shows that this is valid at lower temperatures only. Furthermore, the concentrations' profiles

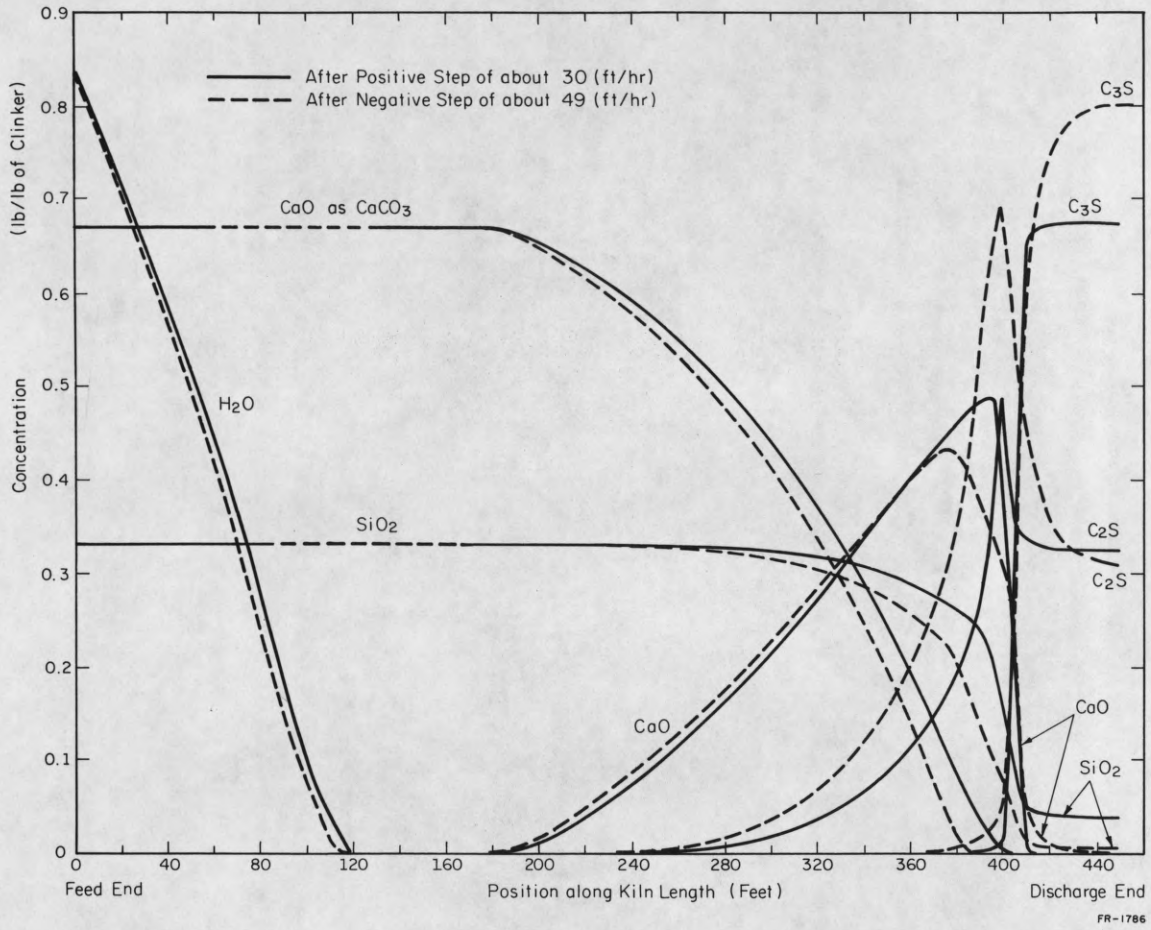

Figure 5. Steady-state concentration profiles after positive and negative step inputs to velocity of the solids.

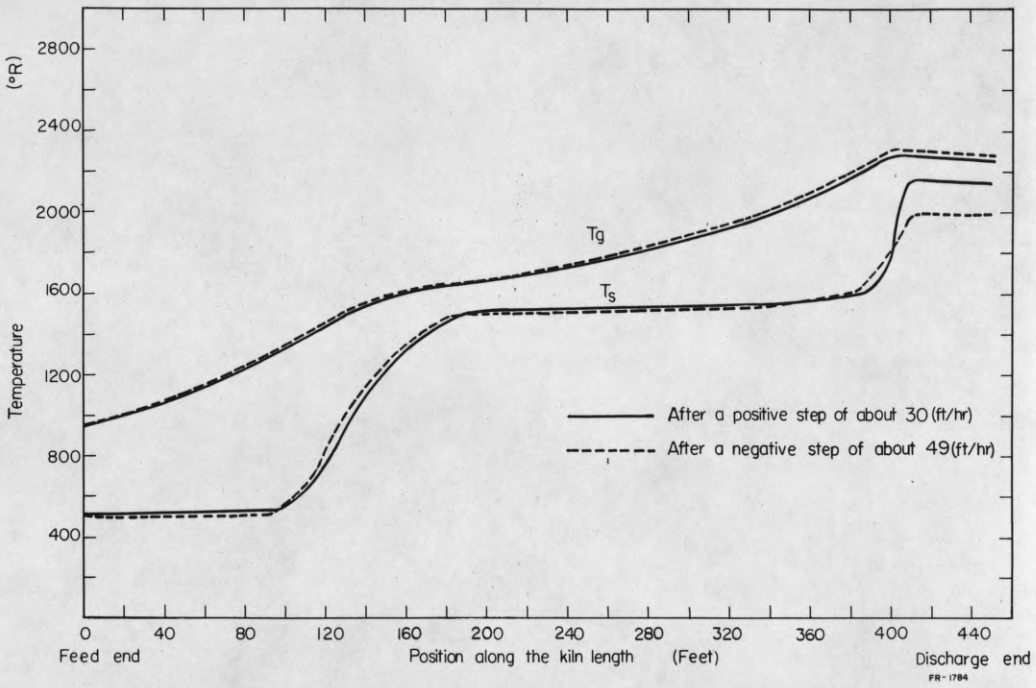

Figure 6. Steady-state temperature profiles after positive and negative step inputs to velocity of the solids.

(see Fig. 5) indicate a strong interaction among process variables at high temperatures, and particularly in the sintering (or burning) zone the effect is very much pronounced. The deterioration in the quality of the end product is also quite obvious. For example, whereas with a normal kiln rotational speed of about 75 (secs/rev) (and hence with the residence time of slurry as 3.5 hours), the C_3S and C_2S concentrations are 0.703 (lb/lb of clinker) and 0.331 (lb/lb of clinker) respectively, the same concentrations radically change to 0.806 (lb/lb of clinker) and 0.308 (lb/lb of clinker) at steady-state after a negative step of $w_o/2.6$, resulting in the kiln rotational speed of 120 (secs/rev) (and hence residence time of slurry as about 5.5 hours). The result is overburnt clinker. Similar analogy shows that with a positive step of $w_o/4.3$, giving a final kiln speed of 60 (sec/rev) (and hence residence time of slurry as only about 2.8 hours), the same concentrations have values of 0.672 (lb/lb of clinker) and 0.326 (lb/lb of clinker) respectively, and the end product is underburnt. But this is of course true when no counteraction is taken simultaneously, i.e. increase or decrease in flow rates of primary and secondary air and fuel to overcome the above effect. This clearly demonstrates the effect of residence time on the quality of the end product, as was mentioned in Section I.2.

The transient shifts in the boundaries of different zones with a positive step of $w_o/4.3$ in the velocity of solids are illustrated in

Figure 7. For the purpose of this analysis, the boundaries were defined as:

$$W[t, L_W(t)] = 0.03 \text{ (lb/lb)} \qquad \text{(end of drying zone)}$$

$$C_1[t, L_{C_1}(t)] = 0.0 \text{ (lb/lb)} \qquad \text{(end of calcining zone)}$$

$$\left.\begin{aligned} S[t, L_S(t)] &= 0.1 \text{ (lb/lb)} \\ X[t, L_X(t)] &= 0.35 \text{ (lb/lb)} \quad \text{and } dX/dL < 0 \\ Y[t, L_Y(t)] &= 0.67 \text{ (lb/lb)} \end{aligned}\right\} \qquad \text{(end of sintering zone)}$$

The family of curves $L = L_j(t)$, obtained by solving the generalized differential-difference equations are shown in Fig. 7. The solutions were obtained by using the numerical method of Runge-Kutta-Gill. From the figure it is observed that the time constants of the curves vary from about 36 mins. to 1 hr. 15 mins., showing that the rotary kiln has an inherent large time lag. It is further clear from the figure that none of the cases exhibit underdamped oscillatory response about their steady-state values. In other words, the system is inherently critically damped (damping ratio = 1.0). The boundary shifts with the positive step were found to be as follows:

Drying zone = 49 ft.

Calcining zone = 46 ft.

Sintering zone = about 42.5 ft. (average of the shifts due to X, Y, and S).

Surprising enough, a negative step in the velocity of solids did not result in any boundary shift. This was quite contrary to the expectations.

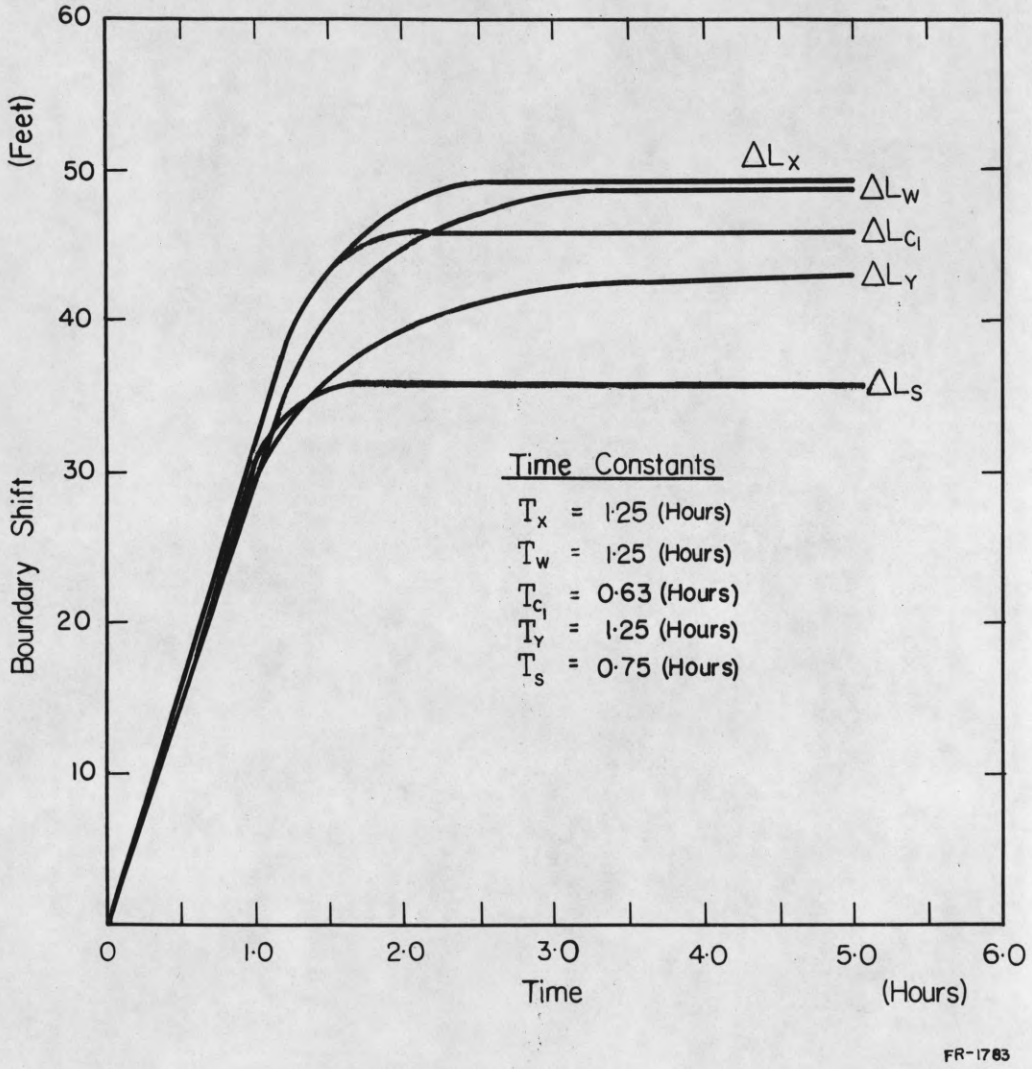

Figure 7. Boundary shifts with a positive step input of 30 (ft/hr) to velocity of the solids.

This transient analysis therefore exhibits some of the practically observed phenomena and gives an insight of the system's dynamic behavior with change in one of the controllable inputs. Further, it helps in predicting some of the control strategies that could be applied to overcome such disturbances. This is briefly discussed in the concluding chapter.

IV. CONCLUSIONS

It has been seen that a rotary kiln is the heart of a cement manufacturing process and that to study its behavior, it is necessary to understand the technology of the process taking place in the kiln.

For the investigation of steady-state and dynamic behaviors of the rotary kiln, first the process variables were defined and then a mathematical model of the process was formulated describing the relationship of those variables. The model essentially represented the material and energy balance at any instant and at any point in the kiln. For this system it was seen that the equations are first-order nonlinear partial differential equations, which were converted to ordinary differential equations for the study of steady-state behavior.

The transient analysis required the division of kiln into a convenient number of small sections of equal lengths and then description of each section by generalized differential-difference equations. Shifts in the boundaries of the zones were obtained for a step change in one of the independent controllable variables, kiln rotational speed (and hence the velocity of the solids in the kiln).

The steady-state and transient models were then simulated on a digital computer and various temperatures and concentration profiles were obtained.

The above indicates how a mathematical model, derived from laws of physics and chemistry, can be used to understand and predict the system behavior under varied conditions. However, a limitation of such a model is that it can only be used for the initial study of the

system behavior under both steady-state and dynamic conditions, and must be suitably modified if it is to be used in implementation of process control. This discrepancy arises in the model used for the study of the rotary kiln because there are no means for on-line analysis of clinker and hence no way to know the dependent variables such as X(t), Y(t), C(t), and Si(t) (see Fig. 3). However, this can be approximately achieved by using clinker density as a quality index.[9,10] The true value of the density can be known only after the clinker is cooled (see Fig. 2) and not as soon as it is discharged from the kiln. This introduces further time lag making the quality control difficult. Because of the difficulty in measuring certain variables of such a mathematical model, new variables can be chosen for actual control purposes. An example of the variables used in actual computer control of a wet process cement rotary kiln,[11] is shown in Figure 8, where the following notation is used:

$r_1(t)$-------- Primary air fan speed (hence flow rate of primary air)

$r_2(t)$-------- Flow rate of fuel

$r_3(t)$-------- Kiln rotational speed

$r_4(t)$-------- Exhaust fan speed (see Fig. 2)

BZT-------- Burning (or sintering) zone temperature

T_g-------- Gas temperature between drying and calcining zones

T_s-------- Solids temperature between drying and calcining zones

t_s-------- Gas temperature in the smoke chamber (see Fig. 2)

AFR-------- Air-fuel ratio

SC-------- Slurry composition (disturbance variable).

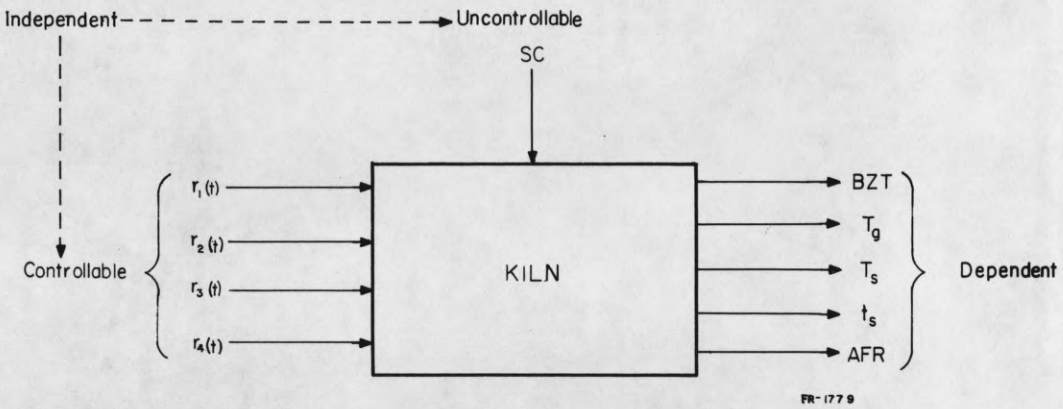

Figure 8. Cement rotary kiln variables used in one of the actual computer control models.

For such a system, however, the process dynamics was approximated by a linear model, the parameters of which were determined by statistical analysis of actual plant operating data.

The transient study can be extended to variations in flow rate of air and fuel. The former can be done by similarly forming differential-difference equations from (II-8) to (II-10) and the latter from (II-13) and (II-14). All these results can then be used to find auto and cross-correlation functions of the various parameters showing mutual dependence of plant processes.

Even though the dynamic behavior with the above variations was not studied, the following predictions can be made as regards the controls that must be applied to the above flow rates if the objective is to maintain the clinker quality.

It has already been seen that reduction in kiln speed results in overburnt clinker and increase in speed yields underburnt clinker, provided no counteraction to overcome the disturbance is taken. The steady-state concentration profiles show that this can be overcome by exercising control over the temperature in the sintering zone, where the interaction of process variables is very much pronounced. The mathematical model indicates that the temperature in this zone is primarily dependent on the fuel and air supply. Thus, the objective can be achieved by decreasing the fuel rate in the former case and increasing the same in the latter. Also, it must be remembered that a change in the fuel rate only would not result in proper combustion unless the air supply is altered simultaneously. This can be best achieved by maintaining a constant air-fuel ratio.

LIST OF REFERENCES

1. V. Filipovich, "Computing Techniques in Automatic Control, Simulation of Transient Processes in Heat Exchangers with Application of Generalized Differential-Difference Equations," Automation and Remote Control, July 1967, pp. 1126-1131, (translated from Avtomatika i Telemekhanika, July 1967, pp. 151-157).

2. E. S. Savas, Computer Control of Industrial Processes, McGraw-Hill Book Co., New York, 1965, pp. 49-54.

3. "Introduction to Control Systems," IBM General Information Manual, 1961, pp. 11.

4. J. W. Lyons, H. S. Mins, P. S. Parisot, and J. Y. Paul, "Experimentation with a Wet-Process Rotary Cement Kiln via Analog Computer," I & EC Process Design and Development, Vol. 1, No. 1, 1962, pp. 29-33.

5. J. W. Lyons, H. S. Mins, P. S. Parisot, and J. Y. Paul, "Computer Simulation of Wet-Process Cement Kiln Operation," ISA Proc. Instrument Automation Conference, Los Angeles, Calif., 1961, preprint 202-LA-61, 1961.

6. A. Sass, "Simulation of Heat Transfer Phenomena in a Rotary Kiln," I & EC Process Design and Development, Vol. 6, No. 4, Oct. 1967, pp. 532-533. See also Vol. 7, No. 2, April 1968, pp. 320.

7. P. V. Varentsov and M. S. Yufa, "Movement of Solid Particle Layers in Rotary Kilns," Chemical Abstracts, Vol. 54, No. 20, 1960, pp. 20362, (original article in Khim Mashinostroenie, No. 5, pp. 22-26, 1959).

8. R. N. Shreve, The Chemical Process Industries, McGraw-Hill Book Co., New York, 1956, pp. 205-215.

9. H. Costa, "Automation of a Rotary Cement Kiln by Means of a Simple Analogue Computer," Automatic and Remote Control, Proc. of First IFAC Congress, Vol. IV, part 3: "Applications," edited by J. F. Coales, Butterworths, London, 1961, pp. 265-273.

10. T. Bay, C. W. Ross, J. C. Andrews, and J. L. Gilliland, "Breakthrough at Tijeras," Leeds and Northrup Technical Journal, Fall issue, 1967, No. 2, pp. 2-15.

11. W. Ostberg, "Computer Ups Cement Production 5 Percent," Control Engineering, Vol. 13, No. 9, 1966, pp. 136-138.

DISTRIBUTION LIST AS OF APRIL 1, 1967

1 Dr. Edward M. Reilley
Asst. Director (Research)
Ofc. of Defense Res. & Engrg.
Department of Defense
Washington, D. C. 20301

1 Office of Deputy Director
(Research and Information Rm. 3D1037)
Department of Defense
The Pentagon
Washington, D. C. 20301

1 Director
Advanced Research Projects Agency
Department of Defense
Washington, D. C. 20301

1 Director for Materials Sciences
Advanced Research Projects Agency
Department of Defense
Washington, D. C. 20301

1 Headquarters
Defense Communications Agency (333)
The Pentagon
Washington, D. C. 20305

50 Defense Documentation Center
Attn: TISIA
Cameron Station, Bldg. 5
Alexandria, Virginia 22314

1 Director
National Security Agency
Attn: TDL
Fort George G. Meade, Maryland 20755

1 Weapons Systems Evaluation Group
Attn: Col. Daniel W. McElwee
Department of Defense
Washington, D. C. 20305

1 National Security Agency
Attn: R4-James Tippet
Office of Research
Fort George G. Meade, Maryland 20755

1 Central Intelligence Agency
Attn: OCR/DD Publications
Washington, D. C. 20505

1 Colonel Kee
AFRSTE
Hqs. USAF
Room 1D-429, The Pentagon
Washington, D. C. 20330

1 Colonel A. Swan
Aerospace Medical Division
Brooks Air Force Base, Texas 78235

1 AUL3T-9663
Maxwell AFB, Alabama 36112

1 AFFTC (FTBPP-2)
Technical Library
Edwards AFB, California 93523

1 Space Systems Division
Air Force Systems Command
Los Angeles Air Force Station
Los Angeles, California 90045
Attn: SSSD

1 Major Charles Waespy
Technical Division
Deputy for Technology
Space Systems Division, AFSC
Los Angeles, California 90045

1 SSD(SSTRT/Lt. Starbuck)
AFUPO
Los Angeles, California 90045

1 Det. #6, OAR (LOOAR)
Air Force Unit Post Office
Los Angeles, California 90045

1 Systems Engineering Group (RTD)
Technical Information Reference Branch
Attn: SEPIR
Directorate of Engineering Standards
& Technical Information
Wright-Patterson AFB, Ohio 45433

1 ARL (ARIY)
Wright-Patterson AFB, Ohio 45433

1 Dr. H. V. Noble
Air Force Avionics Laboratory
Wright-Patterson AFB, Ohio 45433

1 Mr. Peter Murray
Air Force Avionics Laboratory
Wright-Patterson AFB, Ohio 45433

1 AFAL (AVTE/R.D. Larson)
Wright-Patterson AFB, Ohio 45433

2 Commanding General
Attn: STEWS-WS-VT
White Sands Missile Range,
New Mexico 88002

1 RADC (EMLAL-I)
Griffiss AFB, New York 13442
Attn: Documents Library

1 Academy Library (DFSLB)
U. S. Air Force Academy
Colorado Springs, Colorado 80912

1 Lt. Col. Bernard S. Morgan
Frank J. Seiler Research Laboratory
U. S. Air Force Academy
Colorado Springs, Colorado 80912

1 APGC (PGBPS-12)
Elgin AFB, Florida 32542

1 Commanding Officer
Human Engineering Laboratories
Aberdeen Proving Ground, Maryland 21005

1 Director
U. S. Army Engineer Geodesy, Intelligence
and Mapping
Research and Development Agency
Fort Belvior, Virginia 22060

1 Commandant
U. S. Army Command and General Staff College
Attn: Secretary
Fort Leavenworth, Kansas 66270

1 Dr. H. Robl
Deputy Chief Scientist
U. S. Army Research Office (Durham)
Box CM, Duke Station
Durham, North Carolina 27706

1 Commanding Officer
U. S. Army Research Office (Durham)
Attn: CRD-AA-IP (Richard O. Ulsh)
Box CM, Duke Station
Durham, North Carolina 27706

1 Librarian
U. S. Army Military Academy
West Point, New York 10996

1 The Walter Reed Institute of Research
Walter Reed Medical Center
Washington, D. C. 20012

1 Commanding Officer
U. S. Army Electronics R&D Activity
Fort Huachuca, Arizona 85163

1 Commanding Officer
U. S. Army Engineer R&D Laboratory
Attn: STINFO Branch
Fort Belvoir, Virginia 22060

1 Commanding Officer
U. S. Army Electronics R&D Activity
White Sands Missile Range, New Mexico 88002

1 Dr. S. Benedict Levin, Director
Institute for Exploratory Research
U. S. Army Electronics Command
Fort Monmouth, New Jersey 07703

1 Director
Institute for Exploratory Research
U. S. Army Electronics Command
Attn: Mr. Robert O. Parker, Executive
Secretary, JSTAC (AMSEL-XL-D)
Fort Monmouth, New Jersey 07703

1 Commanding General
U. S. Army Electronics Command
Fort Monmouth, New Jersey 07703

Attn: AMSEL-SC
RD-D
RD-G
RD-GF
RD-MAT
XL-D
XL-E
XL-C
XL-S
HL-D
HL-CT-R
HL-CT-P
HL-CT-L
HL-CT-O
HL-CT-I
HL-CT-A
NL-D
NL-A
NL-P
NL-R
NL-S
KL-D
KL-E
KL-S
KL-T
VL-D
WL-D

1 Chief of Naval Research
Department of the Navy
Washington, D. C. 20360
Attn: Code 427

3 Chief of Naval Research
Department of the Navy
Washington, D. C. 20360
Attn: Code 437

2 Naval Electronics Systems Command
ELEX 03
Falls Church, Virginia 22046

1 Naval Ship Systems Command
SHIP 031
Washington, D. C. 20360

1 Naval Ship Systems Command
SHIP 035
Washington, D. C. 20360

2 Naval Ordnance Systems Command
ORD 32
Washington, D. C. 20360

2 Naval Air Systems Command
AIR 03
Washington, D. C. 20360

2 Commanding Officer
Office of Naval Research Branch Office
Box 39, Navy No. 100 F.P.O.
New York, New York 09510

1 AFETR Technical Library
(ETV, MU-135)
Patrick AFB, Florida 32925

1 AFETR (ETLLG-I)
STINFO Officer (For Library)
Patrick AFB, Florida 32925

1 Dr. L. M. Hollingsworth
AFCRL (CRN)
L. G. Hanscom Field
Bedford, Massachusetts 01731

1 AFCRL (CRMXLR)
AFCRL Research Library, Stop 29
L. G. Hanscom Field
Bedford, Massachusetts 01731

1 Colonel Robert E. Fontana
Department of Electrical Engineering
Air Force Institute of Technology
Wright-Patterson AFB, Ohio 45433

1 Colonel A. D. Blue
RTD (RTTL)
Bolling Air Force Base, D. C. 20332

1 Dr. I. R. Mirman
AFSC (SCT)
Andrews AFB, Maryland 20331

1 Colonel J. D. Warthman
AFSC (SCTR)
Andrews AFB, Maryland 20331

1 Lt. Col. J. L. Reeves
AFSC (SCBB)
Andrews AFB, Maryland 20331

2 ESD (ESTI)
L. G. Hanscom Field
Bedford, Massachusetts 01731

1 AEDC (ARO, INC)
Attn: Library/Documents
Arnold AFS, Tennessee 37389

2 European Office of Aerospace Research
Shell Building
47 Rue Cantersteen
Brussels, Belgium

5 Lt. Col. Robert B. Kalisch
Chief, Electronics Division
Directorate of Engineering Sciences
Air Force Office of Scientific Research
Arlington, Virginia 22209

1 U. S. Army Research Office
Attn: Physical Sciences Division
3045 Columbia Pike
Arlington, Virginia 22204

1 Research Plans Office
U. S. Army Research Office
3045 Columbia Pike
Arlington, Virginia 22204

1 Commanding General
U. S. Army Materiel Command
Attn: AMCRD-RS-DE-E
Washington, D. C. 20315

1 Commanding General
U. S. Army Strategic Communications Command
Washington, D. C. 20315

1 Commanding Officer
U. S. Army Materials Research Agency
Watertown Arsenal
Watertown, Massachusetts 02172

1 Commanding Officer
U. S. Army Ballistics Research Laboratory
Attn: V. W. Richards
Aberdeen Proving Ground
Aberdeen, Maryland 21005

1 Commandant
U. S. Army Air Defense School
Attn: Missile Sciences Division, C&S Dept.
P.O. Box 9390
Fort Bliss, Texas 79916

1 Redstone Scientific Information Center
Attn: Chief, Document Section
Redstone Arsenal, Alabama 35809

1 Commanding General
Frankford Arsenal
Attn: SMUFA-1310 (Dr. Sidney Ross)
Philadelphia, Pennsylvania 19137

1 U. S. Army Munitions Command
Attn: Technical Information Branch
Picatinney Arsenal
Dover, New Jersey 07801

1 Commanding Officer
Harry Diamond Laboratories
Attn: Dr. Berthold Altman (AMXDO-TI)
Connecticut Avenue and Van Ness Street, N.W.
Washington, D. C. 20438

1 Commanding Officer
U. S. Army Security Agency
Arlington Hall
Arlington, Virginia 22212

1 Commanding Officer
U. S. Army Limited War Laboratory
Attn: Technical Director
Aberdeen Proving Ground
Aberdeen, Maryland 21005

1 Commanding Officer
Office of Naval Research Branch Office
219 South Dearborn Street
Chicago, Illinois 60604

1 Commanding Officer
Office of Naval Research Branch Office
1030 East Green Street
Pasadena, California 91101

1 Commanding Officer
Office of Naval Research Branch Office
207 West 24th Street
New York, New York 10011

1 Commanding Officer
Office of Naval Research Branch Office
495 Summer Street
Boston, Massachusetts 02210

8 Director, Naval Research Laboratory
Technical Information Officer
Washington, D. C. 20390
Attn: Code 2000

1 Commander
Naval Air Development and Material Center
Johnsville, Pennsylvania 18974

2 Librarian
U. S. Naval Electronics Laboratory
San Diego, California 95152

1 Commanding Officer and Director
U. S. Naval Underwater Sound Laboratory
Fort Trumbull
New London, Connecticut 06840

1 Librarian
U. S. Navy Post Graduate School
Monterey, California 93940

1 Commander
U. S. Naval Air Missile Test Center
Point Mugu, California 95468

1 Director
U. S. Naval Observatory
Washington, D. C. 20390

2 Chief of Naval Operations
OP-07
Washington, D. C. 20350

1 Director, U. S. Naval Security Group
Attn: G43
3801 Nebraska Avenue
Washington, D. C. 20016

2 Commanding Officer
Naval Ordnance Laboratory
White Oak, Maryland 21162

1 Commanding Officer
Naval Ordnance Laboratory
Corona, California 91720

1 Commanding Officer
Naval Ordnance Test Station
China Lake, California 93555

1 Commanding Officer
Naval Avionics Facility
Indianapolis, Indiana 46218

1 Commanding Officer
Naval Training Device Center
Orlando, Florida 32813

1 U. S. Naval Weapons Laboratory
Dahlgren, Virginia 22448

1 Weapons Systems Test Division
Naval Air Test Center
Patuxtent River, Maryland 20670
Attn: Library

1 Head, Technical Division
U. S. Naval Counter Intelligence Support Center
Fairmont Building
4420 North Fairfax Drive
Arlington, Virginia 22203

1 Mr. Charles F. Yost
Special Asst. to the Director of Research
National Aeronautics and Space Administration
Washington, D. C. 20546

1 Dr. H. Harrison, Code RRE
Chief, Electrophysics Branch
National Aeronautics and Space Administration
Washington, D. C. 20546

1 Goddard Space Flight Center
National Aeronautics and Space Administration
Attn: Library C3/TDL
Green Belt, Maryland 20771

1 NASA Lewis Research Center
Attn: Library
21000 Brookpark Road
Cleveland, Ohio 44135

1 National Science Foundation
Attn: Dr. John R. Lehmann
Division of Engineering
1800 G Street, N.W.
Washington, D. C. 20550

1 U. S. Atomic Energy Commission
Division of Technical Information Extension
P. O. Box 62
Oak Ridge, Tennessee 37831

1 Los Alamos Scientific Laboratory
Attn: Reports Library
P. O. Box 1663
Los Alamos, New Mexico 87544

2 NASA Scientific & Technical Information Facility
Attn: Acquisitions Branch (S/AK/DL)
P. O. Box 33
College Park, Maryland 20740

1 Director
Research Laboratory of Electronics
Massachusetts Institute of Technology
Cambridge, Massachusetts 02139

1 Polytechnic Institute of Brooklyn
55 Johnson Street
Brooklyn, New York 11201
Attn: Mr. Jerome Fox
Research Coordinator

1 Director
Columbia Radiation Laboratory
Columbia University
538 West 120th Street
New York, New York 10027

1 Director
Coordinated Science Laboratory
University of Illinois
Urbana, Illinois 61801

1 Director
Stanford Electronics Laboratories
Stanford University
Stanford, California 94305

1 Director
Electronics Research Laboratory
University of California
Berkeley, California 94720

1 Director
Electronic Sciences Laboratory
University of Southern California
Los Angeles, California 90007

1 Professor A. A. Dougal, Director
Laboratories for Electronics and Related Sciences Research
University of Texas
Austin, Texas 78712

1 Division of Engineering and Applied Physics
210 Pierce Hall
Harvard University
Cambridge, Massachusetts 02138

1 Aerospace Corporation
P. O. Box 95085
Los Angeles, California 90045
Attn: Library Acquisitions Group

1 Professor Nicholas George
California Institute of Technology
Pasadena, California 91109

1 Aeronautics Library
Graduate Aeronautical Laboratories
California Institute of Technology
1201 East California Boulevard
Pasadena, California 91109

1 Director, USAF Project RAND
Via: Air Force Liaison Office
The RAND Corporation
1700 Main Street
Santa Monica, California 90406
Attn: Library

1 The Johns Hopkins University
Applied Physics Laboratory
8621 Georgia Avenue
Silver Spring, Maryland 20910
Attn: Boris W. Kuvshinoff
Document Librarian

1 Hunt Library
Carnegie Institute of Technology
Schenley Park
Pittsburgh, Pennsylvania 15213

1 Dr. Leo Young
Stanford Research Institute
Menlo Park, California 94025

1 Mr. Henry L. Bachmann
Assistant Chief Engineer
Wheeler Laboratories
122 Cuttermill Road
Great Neck, New York 11021

1 School of Engineering Sciences
Arizona State University
Tempe, Arizona 85281

1 University of California at Los Angeles
Department of Engineering
Los Angeles, California 90024

1 California Institute of Technology
Pasadena, California 91109
Attn: Documents Library

1 University of California
Santa Barbara, California 93106
Attn: Library

1 Carnegie Institute of Technology
Electrical Engineering Department
Pittsburgh, Pennsylvania 15213

1 University of Michigan
Electrical Engineering Department
Ann Arbor, Michigan 48104

1 New York University
College of Engineering
New York, New York 10019

1 Syracuse University
Department of Electrical Engineering
Syracuse, New York 13210

1 Yale University
Engineering Department
New Haven, Connecticut 06520

1 Airborne Instruments Laboratory
Deerpark, New York 11729

1 Bendix Pacific Division
11600 Sherman Way
North Hollywood, California 91605

1 General Electric Company
Research Laboratories
Schenectady, New York 12301

1 Lockheed Aircraft Corporation
P. O. Box 504
Sunnyvale, California 94088

1 Raytheon Company
Bedford, Massachusetts 01730
Attn: Librarian

1 Dr. G. J. Murphy
The Technological Institute
Northwestern University
Evanston, Illinois 60201

1 Dr. John C. Hancock, Director
Electronic Systems Research Laboratory
Purdue University
Lafayette, Indiana 47907

1 Director
Microwave Laboratory
Stanford University
Stanford, California 94305

1 Emil Schafer, Head
Electronics Properties Info Center
Hughes Aircraft Company
Culver City, California 90230

Security Classification

DOCUMENT CONTROL DATA - R & D

(Security classification of title, body of abstract and indexing annotation must be entered when the overall report is classified)

1. ORIGINATING ACTIVITY (Corporate author)	2a. REPORT SECURITY CLASSIFICATION
University of Illinois Coordinated Science Laboratory Urbana, Illinois 61801	Unclassified
	2b. GROUP

3. REPORT TITLE

Simulation of a Wet Process Cement Rotary Kiln

4. DESCRIPTIVE NOTES (Type of report and inclusive dates)

5. AUTHOR(S) (First name, middle initial, last name)

Jai Hari Dalmia

6. REPORT DATE	7a. TOTAL NO. OF PAGES	7b. NO. OF REFS
September 1968	49	11

8a. CONTRACT OR GRANT NO.	9a. ORIGINATOR'S REPORT NUMBER(S)
DAAB-07-67-C-0199	
b. PROJECT NO.	R-392
c.	9b. OTHER REPORT NO(S) (Any other numbers that may be assigned this report)
d.	

10. DISTRIBUTION STATEMENT

Distribution of this report is unlimited.

11. SUPPLEMENTARY NOTES	12. SPONSORING MILITARY ACTIVITY
	Joint Services Electronics Program thru U.S. Army Electronics Command Ft. Monmouth, New Jersey 07703

13. ABSTRACT

None

DD FORM 1 NOV 65 1473

Security Classification

14. KEY WORDS	LINK A		LINK B		LINK C	
	ROLE	WT	ROLE	WT	ROLE	WT
Digital						
Simulation						
Cement						
Kiln						